ACS APPLIED MATERIALS & INTERFACES

Research Article

www.acsami.org

Acidity-Mediated, Electrostatic Tuning of Asymmetrically Charged Peptides Interactions with Protein Nanopores

Alina Asandei,[†,#] Mauro Chinappi,[‡,#] Hee-Kyoung Kang,[§] Chang Ho Seo,[∥] Loredana Mereuta,[⊥] Yoonkyung Park,[*,§] and Tudor Luchian[*,⊥]

[†]Department of Interdisciplinary Research, Alexandru I. Cuza University, Iasi, Romania

[‡]Center for Life Nano Science, Istituto Italiano di Tecnologia, Rome, Italy

[§]Department of Biomedical Science and Research Center for Proteineous Materials, Chosun University, Gwangju, South Korea

[∥]Department of Bioinformatics, Kongju National University, Kongju, South Korea

[⊥]Department of Physics, Alexandru I. Cuza University, Iasi, Romania

Supporting Information

ABSTRACT: Despite success in probing chemical reactions and dynamics of macromolecules on submillisecond time and nanometer length scales, a major impasse faced by nanopore technology is the need to cheaply and controllably modulate macromolecule capture and trafficking across the nanopore. We demonstrate herein that tunable charge separation engineered at the both ends of a macromolecule very efficiently modulates the dynamics of macromolecules capture and traffic through a nanometer-size pore. In the proof-of-principle approach, we employed a 36 amino acids long peptide containing at the N- and C-termini uniform patches of glutamic acids and arginines, flanking a central segment of asparagines, and we studied its capture by the α-hemolysin (α-HL) and the mean residence time inside the pore in the presence of a pH gradient across the protein. We propose a solution to effectively control the dynamics of peptide interaction with the nanopore, with both association and dissociation reaction rates of peptide-α-HL interactions spanning orders of magnitude depending upon solution acidity on the peptide addition side and the transmembrane electric potential, while preserving the amplitude of the blockade current signature.

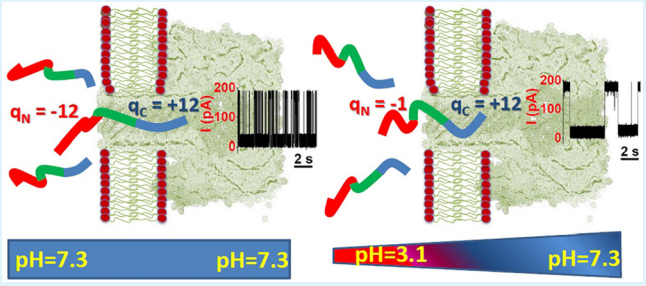

KEYWORDS: *protein nanopore, nanoscale peptide trafficking, single-molecule electrophysiology, lipid bilayer interfaces, biotechnology, control of peptide dynamics*

INTRODUCTION

The transport of proteins or peptides into or across membranes is an essential step for about 50% of the cellular proteins,[1] so that revealing molecular, mechanistic insights into the mechanisms governing the polymer translocation received particular attention in the past years. Arguably, one of the most pressing issues is to understand the biophysical rules that govern the electric field-mediated translocations of peptides through nanopores, by considering the contribution of nonspecific nanopore-polymer interactions.

Synthetic or native nanopores have been endowed in the past two decades with the remarkable ability to probe the transport of various polymer chains at unimolecular level, and this started back in 1996, when the first paper about the possible usefulness of nanopores to DNA probing was published.[2] In principle, the operating principles of the nanopore-based single-molecule technique are elementary simple: the single macromolecule capture, entry and subsequent translocations through a free-standing, voltage-biased nanopore, depend upon the physicochemical and topological features of the analyte. The concentration, identity and other microscopic features of the analyte (e.g., diffusion coefficient, volume, charge, etc.) are inferred from the analysis of the stochastic current blockade events caused by the trafficked analyte across the nanopore.[3−6]

Riding on the current sophistication of electrophysiology technology dedicated to single-molecule detection, either protein- or solid state-based nanopores have emerged as powerful tools for investigation of various chemistries.[7−11] They were also successfully employed for RNA and DNA detection and analysis,[2,12−16] peptides[17−25] or proteins detection and analysis.[26−29]

A wide number of theoretical and computational approaches have been applied to rationalize the analyte capture and translocation[30−33] and to investigate the macromolecule conformation responsible of current alteration at atomic scale.[34−38]

In this context, it is worth mentioning one of the recently introduced, cheap, and easy-to-use devices built around

Received: May 21, 2015
Accepted: July 6, 2015
Published: July 6, 2015

DOI: 10.1021/acsami.5b04406
ACS Appl. Mater. Interfaces 2015, 7, 16706−16714

nanopore technology developed by Oxford Nanopore Technologies (Oxford, UK), MinION, able to reconstruct the nucleotide sequence by quantifying the current fluctuations created when nucleotide strands interact with a protein nanopore during translocation.[39]

To improve the measurement of pico-ampere steps in ion current associated with the transient presence of various molecular moieties within the nanopore, various methods to optimally slow down and control translocation across the nanopore were devised. Among the simplest and less invasive, one could mention altering the temperature, viscosity and salt concentration of the electrolyte,[40,41] the transmembrane potential,[42,43] controlling the balance between the electrostatic and electro-osmotic forces,[22,44,45] employing a pressure-voltage biased pore,[46] or using Li^+ as counterions in the salt solution.[47] Recently, we achieved the simultaneous enhanced sensing throughput and retarded peptide motion across a wild-type α-HL nanopore, by exploiting the electric interaction with the transmembrane potential of neutral homopeptides whose termini were tagged with uniform patches of basic and acid amino acid segments.[48]

In previous reports, authors have demonstrated that electrostatic interactions between the sodium poly(styrenesulfonate) and the α-HL, significantly affects the polymer capture rate and translocation through the protein pore when studied in the presence of various pH and salt gradients.[33,49]

While a complex interplay of fluid dynamics, electrostatic and steric effects govern the peptide-α-HL pore dynamics, we employed herein a 36 amino acids long peptide containing at the N- and C-termini patches of glutamic acids and arginines flanking a central segment of asparagines, to examine the role of the electrostatic contribution to peptides entry to the α-HL, and subsequent trafficking across the nanopore. The parameter used to controllably alter the magnitude of peptide−α-HL interactions was the net charge on the peptide and nanopore, which was varied by exposing a single membrane-immobilized α-HL protein to electrolyte-containing peptides at various acidic pH values, maintained asymmetrical across the nanopore.

EXPERIMENTAL SECTION

Peptide Synthesis. The peptides used herein (Figure 1) are termed CP2a ($Ac-(E)_{12}-(N)_{12}-(R)_{12}-NH_2$), were synthesized by the solid phase method using Fmoc (9-fluorenyl-methoxycarbonyl) chemistry. Their specific length was chosen to ensure that a completely unfolded linear peptide can fit inside the ∼10 nm thick α-HL pore (vide infra). The synthesis protocol, extraction, purification, and molecular mass determination were done as described in detail previously.[48]

Electrophysiology. Planar lipid membranes were obtained employing the Montal−Muller method[19] using 1,2-diphytanoyl-*sn*-glycero-phosphocholine (Avanti Polar Lipids, Alabaster, AL) dissolved in *n*-pentane (HPLC-grade, Sigma-Aldrich, Germany). The dissolved lipid formed stable solventless bilayers across a ∼120 μm in diameter orifice punctured on a 25 μm-thick Teflon film (Goodfellow, Malvern, MA), pretreated with 1:10 hexadecane/pentane (HPLC-grade, Sigma-Aldrich, Germany), that separated the *cis* (grounded) and *trans* chambers of the recording cell. When the experiments were performed in symmetrical conditions, the electrolyte used in both chambers contained 2 M KCl buffered in 10 mM HEPES, at pH = 7.3. For the experiments undertaken in asymmetrical conditions, the electrolyte used in the trans recording chamber contained 2 M KCl buffered in 5 mM MES at pH = 3.73 or 3.17, and that in the grounded *cis* chamber contained 2 M KCl buffered in 10 mM HEPES at pH = 7.3M. All reagents used were of molecular biology purity. A single α-hemolysin protein pore (α-HL) (Sigma-Aldrich, Germany) was inserted in the lipid bilayer by adding ∼0.5−2 μL from a monomeric stock solution made in 0.5 M KCl, to the grounded, *cis* chamber, under continuous stirring for about 5−10 min. The peptide was introduced in *trans* chamber at a bulk concentration of 20 μM from a 1 mM stock solution made in distilled water, and the ion current fluctuations across the α-HL pore reflecting unimolecular reversible interactions between peptides and the α-HL protein were recorded in the voltage-clamp mode with an Axopatch 200B (Molecular Devices, Sunnyvale, CA) amplifier. All experiments were carried out at room temperature of ∼23 °C. Data acquisition was performed with a NI PCI 6221, 16-bit acquisition board (National Instruments, Austin, TX) at a sampling frequency of 50 kHz, within LabVIEW 8.20 (National Instruments, Austin, TX). The amplified electric signals were low-pass filtered at a corner frequency (f_c) of 10 kHz. Numerical analysis and data representations were done with the help of the Origin 6 (OriginLab, Northampton, MA) and pClamp 6.03 (Axon Instruments, Union City, CA) software. The statistical analysis on the relative blockage amplitudes induced by peptides on the electric current through a single α-HL protein, as well as the frequency and duration of the peptides-induced current blockades were analyzed within the statistics of exponentially distributed events, as previously described.[19,22]

Theoretical Model. The theoretical model employed in this paper is based on the toy-model we used in our previous work,[48] here briefly recalled for reader's convenience. We consider only single-file motion, that is, only linear configurations (no hairpin) are allowed inside the pore. Consequently the pore has room for a maximum of 26 residues, roughly corresponding to the pore length L = 100 Å divided by the peptide bond length d_0 = 3.8 Å. Following,[31,50] we indicate as N_{trans} and N_{cis} the number of residues at the *trans* and *cis* side of the pore, and we used $Q = N_{cis} - N_{trans}$ as progress variable to describe the translocation. In particular, $Q = -36$ corresponds to the initial state ($N_{cis} = 0$ and $N_{trans} = 36$) while $Q = 36$ ($N_{cis} = 36$ and $N_{trans} = 0$) corresponds to a complete translocation. A rough estimation of the shape of the free-energy $G(Q)$ can be obtained considering $G(Q)$ as the sum of two independent terms: a configurationally contribution, $G_c(Q)$, and a contribution due to the external electric field, $G_e(Q)$. For the configurationally contribution, as a first approximation, we assume the following form $G_c(Q) = -g\,(N_{cis}\,(Q) + N_{trans}\,(Q))$, where g is a constant with the dimension of an energy.[30,48]

For the electric field contribution, $G_e(Q)$, we consider the work done by the external electric field E acting inside the pore parallel to the pore axis and directed from *trans* to *cis* side.[48] In this study, the new ingredient is given by the dependence on the pH of the peptide N-terminus segment charge. Indicating the *trans* entry as $x = 0$ and the *cis* entry as $x = L$, and denoting by x_t the axial coordinate of the pore below which the peptide charge is affected by the *trans* pH, we assume that the pH inside the pore assumes the *trans* side value for $x < x_t$ and the *cis* side one for $x > x_t$. Consequently, the N-terminus residues with $x < x_t$ has a reduced charge of 0.33 for pH 3.73 and 0.091 for pH = 3.17 (vide infra). Details are reported in Supporting Information. The result reported in this paper are obtained for x_t = 0.25 L. The qualitative picture is not affected by the specific choice for x_t in the range $x_t = [0.1-0.3]$ corresponding to the *trans* portion of the β-barrel (see Supporting Information, Figure S1).

RESULTS

To investigate the modulatory effects exerted by electrostatic forces upon the peptide−α-HL pore interactions, a 2-fold strategy was used: (1) the implication of a peptide able to span the α-HL pore along its entire length, so that while residing inside the pore, the glutamic acids and arginines-containing segments from the peptide's N- and C-termini (Figure 1) most likely face the electrolytes in contact to α-HL's *trans* or *cis* openings, depending upon the peptide orientation within the α-HL, and (2) the use of a pH gradient across the α-HL pore, as to controllably alter the charged state of the α-HL's β-barrel entry and peptide's moieties bathed in the electrolyte in contact

DOI: 10.1021/acsami.5b04406
ACS Appl. Mater. Interfaces 2015, 7, 16706−16714

Figure 1. The primary sequence of the CP2a peptide. Separately, there are displayed the putative charged state of peptide's N- and C-termini in (a) neutral (pH = 7.3), and acidic electrolytes (pH = (b) 3.73 and (c) 3.17).

with the α-HL's β-barrel, while keeping the charge on the protein constriction region and vestibule largely invariant.

In doing so, we generated a biophysical model providing a simplified control over pore-biopolymer interactions, by creating conditions whereby only the electrostatic interactions between the *trans* side exposed protein's β-barrel and either the N- or C-terminus of the peptide segment were modulated controllably via *trans*-pH changes.

To enter the pore from the *trans*-side, a peptide interacts first with the 7-fold symmetric ring from the α-HL's β-barrel mouth, composed of 14 aspartic acids (D127 and D128) and 7 lysines (K131) from the seven protein monomers. Depending on the pH of the *trans* buffer, the net charge of this region on the α-HL (q_{ring}) changes from ~ -7.3 (pH $\sim$ 7.3) to $\sim$0 (pH $\sim$ 3.7), and $\sim$ +6 (pH $\sim$ 3.17),[33] while the charge on the N-terminus of the *trans*-added peptide, changes from $q_N \sim -12$ (pH $\sim$ 7.3) to $q_N \sim -4$ (pH $\sim$ 3.7) and $q_N \sim -1$ (pH $\sim$ 3.1). (http://www.biosyn.com/PeptidePropertyCalculator/PeptidePropertyCalculator.aspx).

The average diameters of the peptide's ends estimated with the Swiss-PdbViewer were $\sim$13.2 Å at the glutamic acids-containing N-terminus and $\sim$18 Å at the arginines-containing C-terminus, while the actual diameter of the α-HL's β-barrel is $\sim$20 Å. At 2 M KCl solution, the Debye length is $\kappa^{-1} \sim 1.9$ Å, which is comparable to the diameter difference between the peptide's N- or C-terminus and pore's β-barrel. With these in mind, and considering the conformational fluctuations of the peptide accompanying its random coil−stretch transition as it enters the pore mouth to enable the eventual single-file trafficking across the pore, one cannot dismiss the manifestations of electrostatic interactions taking place between the peptide and the α-HL's β-barrel. Thus, significant changes in the magnitude of the electrostatic forces manifested between the peptide and the pore ring are expected to occur vs pH, as well as depending on whether the capture of the peptide by the pore takes place on either the N- or C-terminus, all of which should alter distinctly the frequency and duration of peptide-induced blockade events.

Early work has shown that alterations of the pH modifies the electrostatic nature of the α-HL pore, and the peptide or ionic passages through the protein were demonstrated to be controlled by the surface charges of the β-barrel, through changing the solution pH on the trans side of the pore.[22,24,48,51]

Data presented in Figure 2 show that the increase of the *trans* buffer acidity causes a lower propensity of peptide−pore

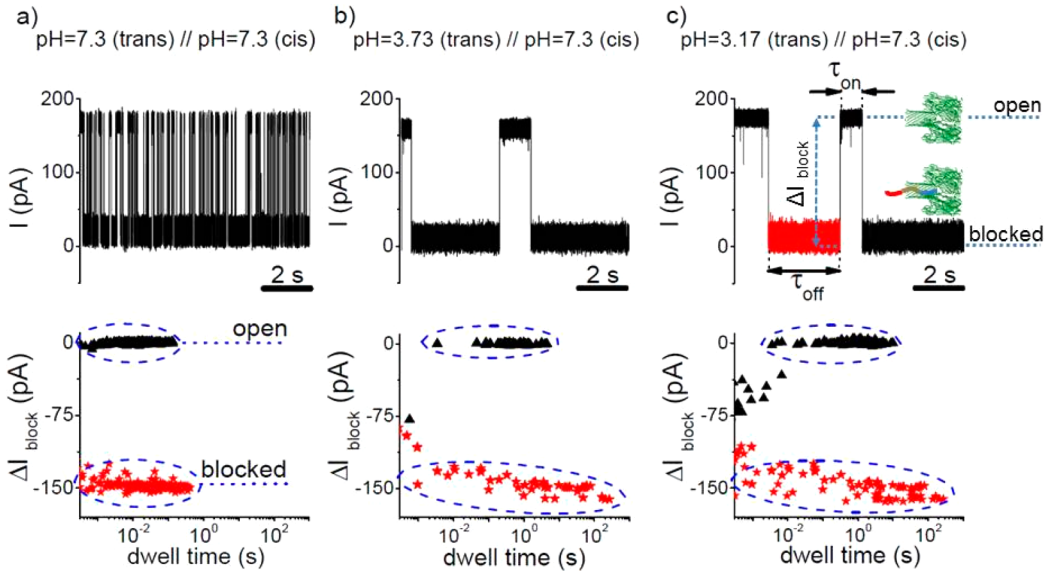

Figure 2. Representative single-pore current recordings reflecting the pH-dependent peptide interaction with the α-HL pore immobilized in a lipid membrane at positive potentials. All traces were recorded with the *trans*-added CP2a peptide (20 μM) at ΔV = +90 mV, in symmetrically added buffer in the *cis* and *trans* chambers containing (a) 2 M KCl, 10 mM HEPES at pH = 7.3 or asymmetrically added buffer (b) 5 mM MES, pH = 3.73(*trans*)/10 mM HEPES, pH = 7.3(*cis*) and (c) 5 mM MES, pH = 3.17(*trans*)/10 mM HEPES, pH = 7.3(*cis*). The reversible peptide-induced blockade events are seen as downward, randomly distributed spikes from the "open" to the "blocked" pore. Scatter plots shown below panels a−c display the interevents (τ_{on}-characteristic of the "open" substate) and blockade (τ_{off}-characteristic of the "closed" substate) dwell times vs relative blockade amplitude of events ($\Delta I_{block} = I_{blocked} - I_{open}$), with the distinct blockade substates encircled. In the scatter plot below panel a, no events with dwell times beyond $\sim$0.5 s were seen. In this case and for the sake of comparison, the scale was extended to up to $\sim$200 s in order to display an axis similar to those in the scatter plots associated with panels b and c.

DOI: 10.1021/acsami.5b04406
ACS Appl. Mater. Interfaces 2015, 7, 16706−16714

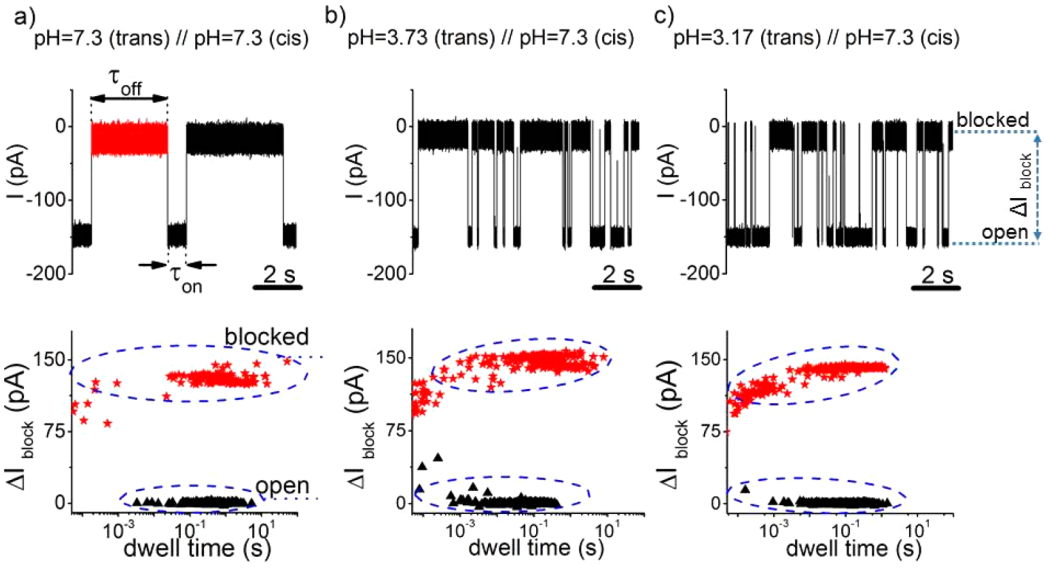

Figure 3. Typical current traces reflecting the pH-dependent peptide interaction with the α-HL pore at negative potentials. In these representative single-pore recordings, the *trans*-added CP2a peptides (20 μM) interacted with a single α-HL protein at $\Delta V = -90$ mV, when both the *cis* and *trans* chambers contained (a) 2 M KCl, 10 mM HEPES at pH = 7.3 or in the presence of asymmetrically added buffer (b) 5 mM MES, pH = 3.73(*trans*)/10 mM HEPES, pH = 7.3(*cis*) and (c) 5 mM MES, pH = 3.17(*trans*)/10 mM HEPES, pH = 7.3(*cis*). The reversible, peptide-induced blockade events are seen as upwardly oriented spikes. Scatter plots of individual, peptide-α-HL reversible interactions are displayed below panels a–c. They quantify the interevents (τ_{on}-characteristic of the "open" substate) and blockade (τ_{off}-characteristic of the "closed" substate) dwell times vs relative blockade amplitude of events (ΔI_{block}) recorded at various *trans* pH values. As in Figure 2, the distinct encircled peaks fingerprint the open pore amplitude and current drop events induced by the peptide–α-HL interactions.

interactions at positively applied potentials, seen as a decrease on the frequency of blockade events. By contrast, when the peptide–pore interactions were studied at negative potentials, an opposite tendency was seen, namely, an increase of the peptide–pore interactions frequency as the *trans*-pH was lowered (Figure 3).

The dissociation times characterizing the reversible α-HL conductance blockades by the CP2a peptide, were also found pH-dependent. At positive potentials applied across the α-HL, *trans*-acidic buffers led to a significant increase of the residence time of a single peptide inside the α-HL pore (Figure 2), while the opposite was measured at negative transmembrane potentials (Figure 3). The subsequent statistical analysis revealed the monoexponential decay-like distributions of interevents and blockade-events durations of peptide-induced α-HL blockades (Supporting Information Figures S2 and S3), which led to the estimation of pH- and voltage-dependence of the association ($rate_{on}$) and dissociation ($rate_{off}$) rates of the CP2a peptide–α-HL interactions. The result of these evaluations is shown in Figure 4, demonstrating that the *trans*-pH controls very effectively the simultaneous enhancement of the peptide capture rate by the α-HL, and peptide residence time within the protein pore, at increasingly either positive or negative transmembrane potentials.

At all pH values of the *trans*-added buffer tested herein, the relative current blockade ΔI_{block} ($\Delta I_{block} = I_{blocked} - I_{open}$) measured versus the transmembrane potential (ΔV) scaled linear with the applied voltage (Figure 5). As we indicated previously,[48] this constitutes proof of the fact that a pore-residing peptide is not being stretched under the influence of the electric field inside the pore, meaning that putative, distinct conformations of peptide inside the pore manifesting at various holding potentials which would alter peptide-pore interactions, cannot account for the difference in $rate_{on}$ and $rate_{off}$ reported in Figure 4.

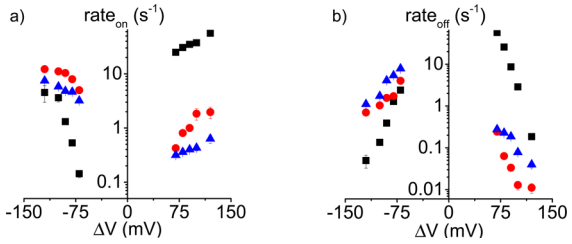

Figure 4. The voltage- and *trans* pH-dependence of the CP2a-α-HL interaction kinetics. The inverse of average time values corresponding to the interevent blockage intervals (τ_{on}) and various peptide-induced blockage levels (τ_{off}) from Figures 2 and 3, provided quantitative estimations of the association ($rate_{on}$) and dissociation ($rate_{off}$) reaction rates characterizing the CP2a–α-HL reversible interactions.[48] The statistical analysis of such data collected over a wide range of the applied transmembrane potential (ΔV), yielded the voltage-dependence of the (a) association ($rate_{on}$) and (b) dissociation ($rate_{off}$) rates during conditions when the pH in the recording chamber was kept symmetrical (■, pH = 7.3(*trans*)/pH = 7.3(*cis*)) or asymmetrical (●, pH = 3.73(*trans*)/pH = 7.3(*cis*); and ▲, pH = 3.17(*trans*) /pH = 7.3(*cis*)).

This observation also justifies the employment of simple model invoked to describing the dynamics of peptide trafficking through α-HL, where the peptide is viewed as an unstructured polymer chain that moves into the pore in "single-file" conformation with no possibility of forming folding intermediates, regardless of the applied voltage (vide infra). However, it is noticeable that the extent of peptide-induced current blockade through the open α-HL pore increases at low pH values (Figure 5), and this indicates that salt ionic passages through a peptide-occupied pore is controlled by the net charges on the pore ring and the peptide.

DOI: 10.1021/acsami.5b04406
ACS Appl. Mater. Interfaces 2015, 7, 16706–16714

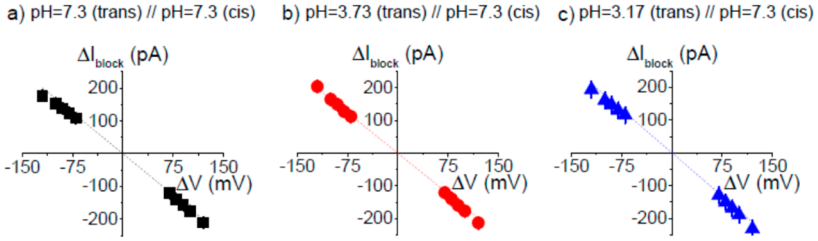

Figure 5. pH-dependence of CP2a peptide-induced blockade amplitude of ion current through an open α-HL. The amplitude of pore-blockade events induced by a peptide trapped inside the α-HL pore ($\Delta I_{block} = I_{blocked} - I_{open}$) showed a linear dependence vs ΔV when the pH in the recording chambers was kept (a) symmetrical (pH = 7.3(*trans*)/pH = 7.3(*cis*)), or asymmetrical ((b) pH = 3.73(*trans*)/pH = 7.3(*cis*)) and (c) pH = 3.17(*trans*)/pH = 7.3(*cis*)). Over the range of the ΔV and pH values used herein, the percentage of the modulus of relative current blockade ($(I_{blocked} - I_{open})/I_{open}$) induced by the pore-residing CP2a peptide was calculated at (a) ΔI % $_{block}$ = 93.5 ± 0.2, (b) ΔI % $_{block}$ = 98.6 ± 0.14, and (c) ΔI % $_{block}$ = 97.1 ± 0.21.

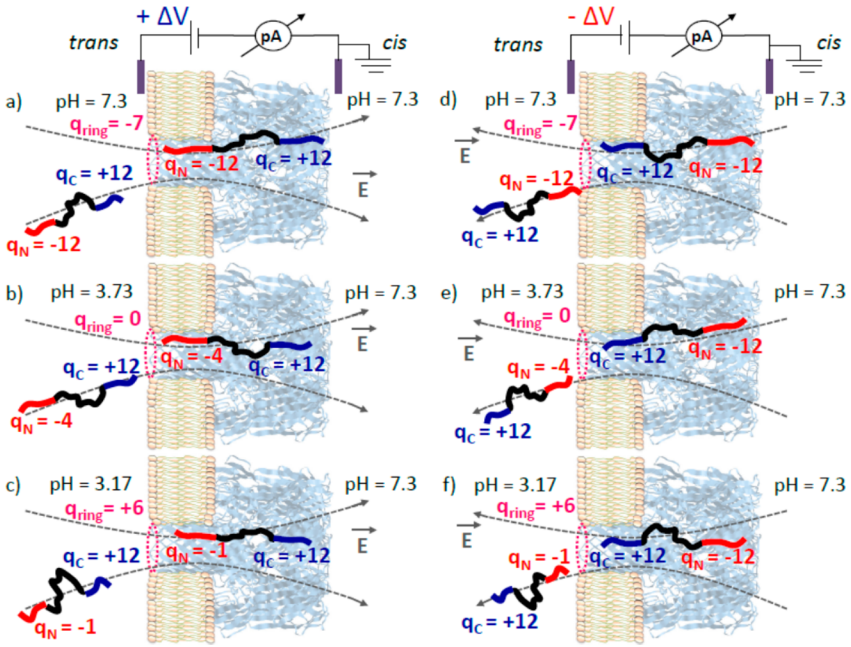

Figure 6. Sketchy representations of the CP2a peptide–α-HL interactions, with either positive or negative transmembrane potentials (ΔV) driving the *trans*-added peptide into the pore. Schematically, we show a single α-HL protein inserted into a lipid bilayer clamped to transmembrane potential, and *trans*-added peptides whose side termini charges are denoted by q_N (N-terminus) and q_C (C-terminus). Depending of the *trans* pH, the net charge of the *trans*-exposed peptide N-terminus (q_N) and α-HL's pore mouth (q_{ring}) changes accordingly. Due to its length, the peptide spans the entire length of the protein pore, so that (a–c) its N- and C-termini are exposed in the vicinity of *trans* and *cis* solutions at $+\Delta V$, while (d–f) the opposite occurs at $-\Delta V$. Consequently, the charged state of the N terminus of nanopore-captured peptide is prone to vary with the pH drop on the *trans*-added electrolyte, only when positive ΔV were used to capture the peptide (see also text).

DISCUSSION

As we did previously,[48] we tackled the voltage-dependence of a peptide association (rate$_{on}$) and the dissociation (rate$_{off}$) rates (Figure 4) measured at neutral pH maintained symmetrically across the α-HL protein, by employing a simplified model—which we imported herein, vide infra—where we assumed a negligible contribution from the electro-osmotic flow through the pore or the effect of the fluid flow outside the pore. This is justified by the lack of secondary structure of peptide confined inside the pore, or some specific folding mediated by adequately spaced amino acids with turn-forming propensity,[22] which would make it more prone to such behavior. In short, depending upon the sign of the applied potential (ΔV), the N- and C-termini charge separation on the CP2a peptide helps the molecule rotate and orient itself along the electric field lines pointing toward the pore *trans* opening, either with the positive tail (at positive ΔV) or negative moiety (at negative ΔV). In the close vicinity of the nanopore, a net dielectrophoretic force acts on the peptide causing the reversible peptide capture by the α-HL, and an increase of the applied voltage (ΔV) irrespective of its sign, causes the electric force acting of the peptide to also increase, hence making capture more probable. Subsequent to peptide entry into the nanopore, the electric force acting at the two oppositely charged peptide termini and the stochastic movement of the peptide resemble a tug of war able to stabilize the peptide inside the pore at increasing transmembrane potentials.[48]

In the light of the findings embodied by Figure 4a, a first compelling question is why *trans*-acidic pH values make the peptide less likely to enter the protein's β-barrel at positive ΔV, while the exact opposite happens at negative ΔV? In concise terms, such results stem from simple electrostatics. Namely, at a positively applied voltage, the *trans*-added peptides are driven toward the nanopore with the C-terminus head-on (vide infra),

DOI: 10.1021/acsami.5b04406
ACS Appl. Mater. Interfaces 2015, 7, 16706–16714

so that the positive charges of the peptide's C-terminus moiety face the negative charges of the α-HL's ring. Increasing *trans*-solution acidity neutralizes these negative charges on the protein's β-barrel entry, reducing the peptide-channel attractive interaction. On the contrary, at a negatively applied voltage the *trans*-added peptides are driven toward the nanopore with negatively charged N-terminus head-on (vide infra), and encounter the negative charges of the α-HL's ring. Therefore, increasing *trans*-solution acidity neutralizes negative charges in both the peptide's N-terminus moiety and the α-HL's ring, reducing the mutual repulsion and making the peptide more likely to enter the pore.

To also provide a comprehensive interpretation the pH-dependent dissociation rates ($rate_{off}$) reported in Figure 4b, we supplement the above-mentioned mechanistic description with the following hypotheses: (1) The charged state of the α-HL's trans opening (q_{ring}) varies vs *trans* pH as indicated before,[33] and represented in Figure 6. (2) The charged state of the α-HL's constriction and vestibule regions remains invariant vs pH changes imposed in the *trans* side. This is mainly because the α-HL is anionic selective, its selectivity gets augmented at more acidic pH values,[22] so that entry of protons into the pore does not make a sizable difference in terms of altering the protonation state of the constriction- or vestibule-located residues, at least within the relative short durations of the experiments. (3) At positively applied potentials, the *trans*-added peptides are driven toward the nanopore with the C-terminus head-on (Figure 6a−c). Once it gets temporarily trapped inside the α-HL and due to the peptide length, the N-terminus part of the peptide remains exposed to the *trans* side of the membrane (Figure 6a−c), so its protonation state and net charge will change depending upon the *trans*-pH, as depicted in Figure 1. (4) At negatively applied potentials and all pH tested, the *trans*-added peptides are driven toward the nanopore with negatively charged N-terminus head-on (Figure 6d−f). Due to geometric considerations, a peptide trapped inside the α-HL at negative ΔV, is capable of reaching the *cis* side of the membrane with its N-terminus moiety, and its protonation state would resemble that encountered at neutral pH (i.e., the pH of the *cis* side), thus becoming unaffected by the *trans* acidic pH (Figure 6d−f).

With these in mind, we provide below an interpretation the pH-dependent, association ($rate_{on}$) and dissociation ($rate_{off}$) rates reported in Figure 4, for both positive and negative potentials.

***Trans* pH- and Transmembrane Potential Dependence of CP2a Peptide-α-HL Association Rates.** For the experimental assembly presented herein, the *trans* pH acts in two different ways. On the one hand it alters the protein's ring charge (q_{ring}), and in particular the *trans* entry of the α-HL changes its charged state from net negative at neutral pH, to almost zero at pH = 3.73 and net positive at pH = 3.17. On the other hand, the *trans* pH induces a charge asymmetry on the peptide chain, which goes from overall neutral at pH 7.3 (N-terminus charge $q_N \sim -12$, C-terminus charge $q_C \sim +12$, Figure 1a) to strongly asymmetrical at pH = 3.73, where $q_N \sim -4$ and $q_C \sim +12$ (Figure 1b) and pH = 3.17, where $q_N \sim -1$ and $q_C \sim +12$ (Figure 1c).

These two effects play an opposite role in the pH dependency of the peptide association rate to the α-HL pore ($rate_{on}$). That is, as pH decreases, the peptide becomes more positively charged, hence at positive ΔV the small but non negligible electrical field (E) on the *trans* side vicinity of the α-HL would facilitate peptides entry into the α-HL pore. Hence, decreasing the *trans* pH, would entail an increase of the $rate_{on}$. At the same time, however, the pH-dependent ring charge on the protein affects $rate_{on}$ in the opposite way. As evidenced above, q_{ring} changes from net negative at pH = 7.3 to net positive at pH = 3.17, thus constituting an electrostatic barrier for the peptides which are driven with the positive C-terminus tail toward the pore by positive ΔV , at such acidic pH values (Figure 6a−c). The experimental data indicate that this latter effect is dominant, leading to a corresponding decrease in the peptide association rate to the nanopore with a decrease in the *trans* pH (Figure 4a).

Trans-negative potentials drive the peptides toward the nanopore mouth with the negatively charged N-terminus head-on (Figure 6d−f). Given that the net negative charge on the N-terminus segment decreases with the drop in the *trans*-pH, and so does the magnitude of the electrophoretic force which imports the peptide to the pore entry, the expectation would be that the peptide capture rate decreases with the pH drop. Paradoxically, the opposite occurs, as the data shown in Figure 4a demonstrates. By following a similar line of reasoning as above, we posit that when the α-HL is held at negative ΔV , increasingly acidic *trans* buffers lower both the q_N as well as q_{ring}, and so electrostatic attractions of incoming peptides to the pore mouth will manifest below pH = 3.73 (Figure 6d−f). Consequently, the climbing potential barrier for peptide entry inside the pore—which involves among others the entropy penalty for orienting the peptide chain and its interactions with polarization-induced charges at the water-membrane interface—gets lowered. Thus, the overall the free energy barrier for peptide entry to the pore is decreased when the *trans*-pH is lowered, making the peptide entry into the β-barrel more probable. Within such a simplified rationale, however, one would expect that the $rate_{on}$ of peptide−α-HL interactions would be larger at a *trans* pH = 3.17 than that at *trans* pH = 3.73, and this is in contrast with our findings (Figure 4a). The nonmonotonic behavior of CP2a $rate_{on}$ vs *trans* pH measured at negative ΔV is still under investigation in our laboratories. So far, it indicates the nontrivial interplay between the $q_N - q_{ring}$ electrostatic interactions and peptide-transmembrane electrical field interactions, in setting the propensity of peptide capture rate by the α-HL pore.

***Trans* pH- and Transmembrane Potential Dependence of CP2a Peptide-α-HL Dissociation Rates.** To rationalize the dynamics of the CP2a peptide across the α-HL pore, at distinct *trans* pH values and applied transmembrane potentials (ΔV), we note that at positive ΔV, a pore-captured peptide still exposes its N-terminal in the close vicinity of the membrane *trans* side, so that increasingly acidic *trans* buffers would increase the peptide's N-terminal moiety electrostatic attraction to the increasingly positive charged β-barrel mouth of the α-HL (Figure 6, panels a, b and c). While at pH = 7.3 the interaction between a α-HL-captured peptide and the pore itself is repulsive ($q_{ring} = -7$ and $q_N = -12$) (Figure 6, panel a), by lowering the *trans* pH below 3.73, such interactions become attractive (Figure 6, panel c), thus making the peptide harder to leave the protein's β-barrel. Hence, on the sole basis of ring charge, the peptide dissociation rate should decrease with a drop in *trans* pH. In light of our experiments however, this prediction is only partially met, since according to the rationale presented above, the decrease in $rate_{off}$ vs pH at positively applied potentials should be more prevalent at pH 3.17 than pH 3.73, which is not the case (see Figure 4, panel b).

DOI: 10.1021/acsami.5b04406
ACS Appl. Mater. Interfaces 2015, 7, 16706−16714

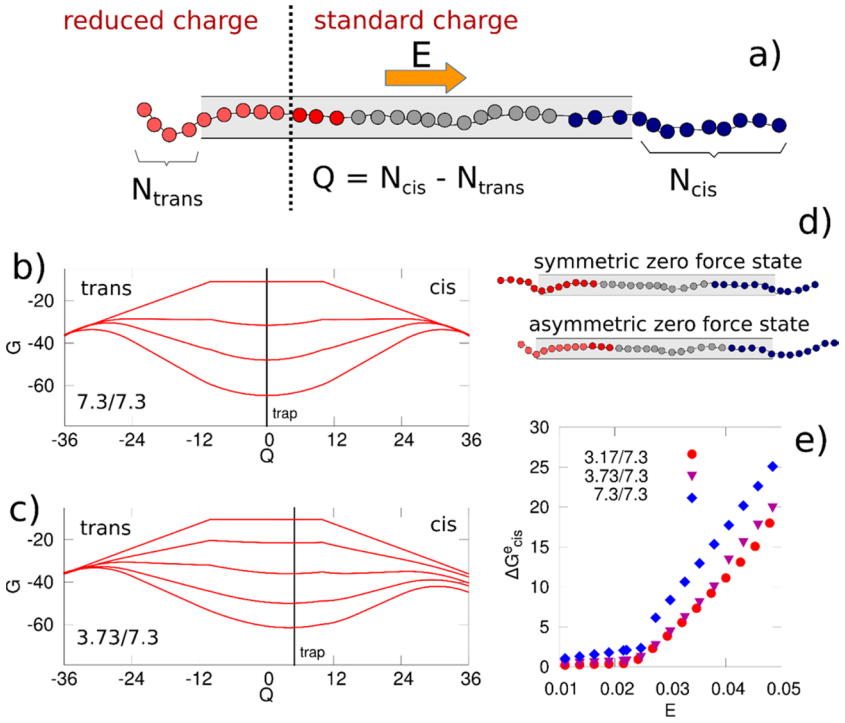

Figure 7. Sketch of the toy model for positive applied potential. Only the charge asymmetry effect is considered. The charge of the residues belonging to the negative tail is reduced when the residue is at the *trans*-entry, whereas when a residue moves toward the *cis* side, the standard charge is recovered (panel a). Panels b and c report the free-energy profiles for the symmetrical (pH = 7.3(*trans*)/pH = 7.3(*cis*)) or asymmetrical (pH = 3.73(*trans*)/pH = 7.3(*cis*) case. It is apparent that the zero-force state is shifted toward the *cis* side. In panel d, a cartoon representation of the peptide inside the pore with the configurations of the zero force state, with the pore exposed to symmetric and asymmetric pH, is shown. Panel e reports the escape barrier as a function of the electrical field for different *trans* pH. For the sake of completeness, results for negative potentials are reported in the Supporting Information, Figure S4.

To explain this, we need to take into account the pH-dependent charge asymmetry buildup on the peptide. To start with, note that the charged residues from the N- and C-termini of a pore-trapped peptide experience additional electrical forces from the interaction with the transmembrane potential. The metastability of the peptide trapped inside the α-HL pore is crucially determined by the electrostatic forces acting on the both ends of the peptide, which must be equal in absolute values and act oppositely in order to enable lower values for the peptide dissociation rate from the pore.[48] In our case, at $+\Delta V$, lower *trans* pH values lead to an unbalance of the net charge present of the pore-captured peptide termini (see Figure 6, panels b and c), so that the peptide would sense asymmetrical forces acting oppositely onto its C- and N-termini from the transmembrane electric field. This phenomenon is expected to be more prevalent at pH = 3.17 (N-terminus charge $(q_N) \sim -1$, C-terminus charge $(q_C) \sim +12$) as compared to pH = 3.73 (N-terminus charge ~ -4, C-terminus charge $\sim +12$). As a result, at a *trans* pH = 3.17 and positively applied potentials, the *trans* to *cis* oriented, net electric force, acting on the poreconfined peptide, is larger than that which manifests under otherwise similar conditions, but a *trans* pH = 3.73.

We conjecture that at $+\Delta V$, the more destabilizing, net electric force acting of the poreconfined peptide at a *trans* pH = 3.1 as compared to pH = 3.7, may decompensate the stabilizing effect mediated by the augmented electrostatic interactions between the peptide's N-terminal and the pore's *trans* opening, which tend to be more prevalent at pH = 3.17 than pH = 3.7 (vide supra). Consequently, at $+\Delta V$ the α-HL trapped peptide would become more prone to exiting the pore when the *trans* pH equals 3.17 than 3.73.

This qualitative explanation can be also formalized using a simple toy-model we already employed[48] where the free-energy profile of the peptide translocation is calculated. Figure 7, panel a reports the schematic representation of the theoretical toy-model. The pore is assumed to be cylindrical, the peptide is linear and the electrical field acts only on the residues inside the pore. The charge of the N-terminus residues is assumed to depend on the position of the residue in the pore. In particular, the charge is reduced in the *trans* region, i.e. when pH is lower (see the Experimental Section). Figure 7, panels b and c report the free energy profile as a function of the collective variable Q ($Q = -36$ means that the whole chain in on the *trans* side, while $Q = 36$ corresponds to the peptide completely translocated) for the case *trans* pH = 7.3 and *trans* pH = 3.7. As expected, the zero force state is shifted toward the *cis* side (see also in Figure 7, panel d). Moreover, the escape barrier, i.e. the difference between the free-energy minimum and the maximum at the *trans* side, is lower (Figure 7, panel e).

In summary, at positive ΔV, the α-HL trapped peptide would become more prone to exiting the pore when the *trans* pH decreases. In direct connection to this interpretation, it must be remarked that previously we tested the crucial role played by un-balanced electric forces acting on the N- and C-terminal of a pore-residing peptide on its dissociation rate from the pore, by devising working conditions whereby such forces were altered distinctly by imposing a salt concentration gradient across the α-HL pore, while maintaining the charged state of the peptide invariant.[48] For the case of negative applied transmembrane

DOI: 10.1021/acsami.5b04406
ACS Appl. Mater. Interfaces 2015, 7, 16706−16714

potentials, the conciliation of experimental data with the theoretical paradigm presented above is easier to reach, since the peptide charge asymmetry vs *trans* pH becomes less relevant. That is, as a peptide gets trapped inside the pore, its N-terminal segment will reach to the *cis* chamber (pH = 7.3) and consequently the net charge changes to a value of $q_N \sim -12$ encountered around neutral pH (Figure 6, panels d, e and f). We propose that for a peptide captured inside the α-HL pore that at $-\Delta V$, *trans* pH values will alter the peptide dynamics inside the pore solely by tuning the electrostatic interactions manifested between the *trans* pH-dependent pore's mouth (q_{ring}) and the C-terminal of the poretrapped peptide (q_C), which become less attractive when more acidic as compared to neutral pH. Thus, electrostatic interactions manifested between the pore's mouth and peptide's C-terminus would more likely facilitate peptide passage at *trans* pH 3.17 than at pH 3.73. As shown in Figure 4, panel b, this prediction is nicely met by the experimental data, which demonstrate that the peptide passage rate across the pore (rateoff) gets augmented in the presence of *trans* acidic electrolytes and $-\Delta V$.

CONCLUDING REMARKS AND FUTURE PROSPECTS

In this study, we set up an experimental biophysical model providing a simplified control over α-HL−peptide interactions. The main ingredient was the use of neutral homopeptides containing oppositely charged amino acid patches at the N- and C-termini, able to span a single α-HL protein immobilized on a lipid membrane. This study complements previous efforts from our groups regarding the elucidation of pH- and ionic strength-induced modulations of inter-residues electrostatic interactions, on the dynamics of histidine-containing peptides interacting with the α-HL protein.[24]

The main finding of this study is that by changing the pH of the solution in contact to the α-HL's β-barrel opening from neutral to more acidic values, one is able to modulate the electrostatic interactions between the protein's mouth and either the N- or C-terminus end of the peptide. This is indicative of an effective method of controlling single peptide interaction with and passage through nanopore, preserving at the same time the signal blockade amplitudes.

The major advantages of the presented approach, which can be easily extended to other biological polymers, are (1) the asymmetric charge distribution at the peptide N- and C-termini, helps the peptide rotate and orient itself as to facilitate its capture and subsequent threading inside the α-HL pore irrespective of the transmembrane potential sign, and (2) the pH-adjustable charge distribution on the peptide and nanopore allow the convenient, electrostatic tuning of peptide capture by the nanopore and its subsequent dynamics inside the nanopore.

By creating conditions whereby during the same experiment, peptide entry into the nanopore can be set from the sign of the applied transmembrane potential to occur with either N- or C-terminus end head-on, an additional control of electrostatic interactions between the pH-dependent, charged peptide moieties and the nanopore can be achieved. This approach provides essential benefits to the requirements of optimal time and signal resolution, controllable solely by pH and trans-membrane potentials and combined with mutagenesis design strategies to rationally alter the electrostatic landscape along the nanopore walls,[52] it may be useful for the task of polymer sequencing.

ASSOCIATED CONTENT

Supporting Information

Explicit expression for the electrical field contribution to the free-energy profile for the toy-model employed to describe the α-HL-CP2a interaction and dwell-time histogram analysis of representative electrophysiology traces showing the reversible α-HL-CP2a interaction. The Supporting Information is available free of charge on the ACS Publications website at DOI: 10.1021/acsami.5b04406.

AUTHOR INFORMATION

Corresponding Authors

*E-mail: y_k_park@chosun.ac.kr.
*E-mail: luchian@uaic.ro.

Author Contributions

#These authors contributed equally to this work.

Notes

The authors declare no competing financial interest.

ACKNOWLEDGMENTS

The authors acknowledge the financial support offered by grants PN-II-ID-PCCE-2011-2-0027, PN-II−PT-PCCA-2011-3.1-0595, PN-II−PT-PCCA-2011-3.1-0402, the National Research Foundation of Korea (NRF) grant funded by the Korea government (MEST) (No. 2011-0017532) and Global Research Laboratory (GRL) Grant (NRF-2014K1A1A2064460).

REFERENCES

(1) Harsman, A.; Kruger, V.; Bartsch, P.; Honigmann, A.; Schmidt, O.; Rao, S.; Meisinger, C.; Wagner, R. Protein Conducting Nanopores. *J. Phys.: Condens. Matter* **2010**, *22*, 454102.
(2) Kasianowicz, J. J.; Brandin, E.; Branton, D.; Deamer, D. W. Characterization of Individual Polynucleotide Molecules Using a Membrane Channel. *Proc. Natl. Acad. Sci. U. S. A.* **1996**, *93*, 13770−13773.
(3) Majd, S.; Yusko, E. C.; Billeh, Y. N.; Macrae, M. X.; Yang, J.; Mayer, M. Applications of Biological Pores in Nanomedicine, Sensing, and Nanoelectronics. *Curr. Opin. Biotechnol.* **2010**, *21*, 439−476.
(4) Wang, G.; Wang, L.; Han, Y.; Zhou, S.; Guan, X. Nanopore Stochastic Detection: Diversity, Sensitivity, and Beyond. *Acc. Chem. Res.* **2013**, *46*, 2867−2877.
(5) Gu, L. Q.; Shim, J. W. Single Molecule Sensing by Nanopores and Nanopore Devices. *Analyst* **2010**, *135*, 441−451.
(6) Kasianowicz, J. J.; Robertson, J. W. F.; Chan, E. R.; Reiner, J. E.; Stanford, V. M. Nanoscopic Porous Sensors. *Annu. Rev. Anal. Chem.* **2008**, *1*, 737−766.
(7) Luchian, T.; Shin, S. H.; Bayley, H. Single-Molecule Covalent Chemistry with Spatially Separated Reactants. *Angew. Chem., Int. Ed.* **2003**, *42*, 3766−3771.
(8) Shin, S. H.; Luchian, T.; Cheley, S.; Braha, O.; Bayley, H. Kinetics of a Reversible Covalent-Bond-Forming Reaction Observed at the Single-Molecule Level. *Angew. Chem., Int. Ed.* **2002**, *41*, 3707−3709.
(9) Gu, L. Q.; Braha, O.; Conlan, S.; Cheley, S.; Bayley, H. Stochastic Sensing of Organic Analytes by a Pore-Forming Protein Containing a Molecular Adapter. *Nature* **1999**, *398*, 686−690.
(10) Asandei, A.; Mereuta, L.; Luchian, T. The Kinetics of Ampicillin Complexation by gamma-Cyclodextrins. A Single Molecule Approach. *J. Phys. Chem. B* **2011**, *115*, 10173−10181.
(11) Asandei, A.; Apetrei, A.; Luchian, T. Uni-Molecular Detection and Quantification of Selected beta-Lactam Antibiotics with a Hybrid alpha-Hemolysin Protein Pore. *J. Mol. Recognit.* **2011**, *24*, 199−207.
(12) Akeson, M.; Branton, D.; Kasianowicz, J. J.; Brandin, E.; Deamer, D. W. Microsecond Time-Scale Discrimination among Polycytidylic Acid, Polyadenylic Acid, and Polyuridylic Acid as

DOI: 10.1021/acsami.5b04406
ACS Appl. Mater. Interfaces 2015, 7, 16706−16714

Homopolymers or as Segments within Single RNA Molecules. *Biophys. J.* **1999**, *77*, 3227−3233.
(13) Wanunu, M. Nanopores: A Journey towards DNA Sequencing. *Phys. Life Rev.* **2012**, *9*, 125−158.
(14) Meller, A.; Nivon, L.; Brandin, E.; Golovchenko, J.; Branton, D. Rapid Nanopore Discrimination between Single Oligonucleotide Molecules. *Proc. Natl. Acad. Sci. U. S. A.* **2000**, *97*, 1079−1084.
(15) Astier, Y.; Braha, O.; Bayley, H. Toward Single Molecule DNA Sequencing: Direct Identification of Ribonucleoside and Deoxyribonucleoside 5′-Monophosphates by Using an Engineered Protein Nanopore Equipped with a Molecular Adapter. *J. Am. Chem. Soc.* **2006**, *128*, 1705−1710.
(16) Ashkenasy, N.; Sanchez-Quesada, J.; Bayley, H.; Ghadiri, M. R. Recognizing a Single Base in an Individual DNA Strand: a Step toward DNA Sequencing in Nanopores. *Angew. Chem., Int. Ed.* **2005**, *44*, 1401−1404.
(17) Movileanu, L.; Schmittschmitt, J. P.; Scholtz, J. M.; Bayley, H. Interactions of Peptides with a Protein Pore. *Biophys. J.* **2005**, *89*, 1030−1045.
(18) Stefureac, R.; Long, Y. T.; Kraatz, H. B.; Howard, P.; Lee, J. S. Transport of α-Helical Peptides through α-Hemolysin and Aerolysin Pores. *Biochemistry* **2006**, *45*, 9172−9179.
(19) Asandei, A.; Apetrei, A.; Park, Y.; Hahm, K. S.; Luchian, T. Investigation of Single-Molecule Kinetics Mediated by Weak Hydrogen-Bonds within a Biological Nanopore. *Langmuir* **2011**, *27*, 19−24.
(20) Mereuta, L.; Schiopu, I.; Asandei, A.; Park, Y.; Hahm, K. S.; Luchian, T. Protein Nanopore-Based, Single-Molecule Exploration of Copper Binding to an Antimicrobial-Derived, Histidine-Containing Chimera Peptide. *Langmuir* **2012**, *28*, 17079−17091.
(21) Asandei, A.; Schiopu, I.; Iftemi, S.; Mereuta, L.; Luchian, T. Investigation of Cu2+ Binding to Human and Rat Amyloid Fragments Aβ (1−16) with a Protein Nanopore. *Langmuir* **2013**, *29*, 15634−15642.
(22) Mereuta, L.; Roy, M.; Asandei, A.; Lee, J. K.; Park, Y.; Andricioaei, I.; Luchian, T. Slowing Down Single-Molecule Trafficking through a Protein Nanopore Reveals Intermediates for Peptide Translocation. *Sci. Rep.* **2014**, *4*, 3885.
(23) Asandei, A.; Iftemi, S.; Mereuta, L.; Schiopu, I.; Luchian, T. Probing of Various Physiologically Relevant Metals-Amyloid-β Peptide Interactions with a Lipid Membrane-Immobilized Protein Nanopore. *J. Membr. Biol.* **2014**, *247*, 523−530.
(24) Mereuta, L.; Asandei, A.; Seo, C. H.; Park, Y.; Luchian, T. Quantitative Understanding of pH- and Salt-Mediated Conformational Folding of Histidine-Containing, β-Hairpin-Like Peptides, through Single-Molecule Probing with Protein Nanopores. *ACS Appl. Mater. Interfaces* **2014**, *6*, 13242−13256.
(25) Wang, H. Y.; Ying, Y. L.; Li, Y.; Kraatz, H. B.; Long, Y. T. Nanopore Analysis of β-Amyloid Peptide Aggregation Transition Induced by Small Molecules. *Anal. Chem.* **2011**, *83*, 1746−1752.
(26) Han, A.; Creus, M.; Schurmann, G.; Linder, V.; Ward, T. R.; de Rooij, N. F.; Staufer, U. Label-Free Detection of Single Protein Molecules and Protein-Protein Interactions Using Synthetic Nanopores. *Anal. Chem.* **2008**, *80*, 4651−4658.
(27) Oukhaled, G.; Mathé, J.; Biance, A. L.; Bacri, L.; Betton, J. M.; Lairez, D.; Pelta, J.; Auvray, L. Unfolding of Proteins and Long Transient Conformations Detected by Single Nanopore Recording. *Phys. Rev. Lett.* **2007**, *98*, 158101.
(28) Oukhaled, A.; Bacri, L.; Pastoriza-Gallego, M.; Betton, J. M.; Pelta, J. Sensing Proteins through Nanopores: Fundamental to Applications. *ACS Chem. Biol.* **2012**, *7*, 1935−1949.
(29) Talaga, D. S.; Li, J. Single-molecule Protein Unfolding in Solid State Nanopores. *J. Am. Chem. Soc.* **2009**, *131*, 9287−9297.
(30) Muthukumar, M. Theory of Capture Rate in Polymer Translocation. *J. Chem. Phys.* **2010**, *132*, 195101.
(31) Bacci, M.; Chinappi, M.; Casciola, C. M.; Cecconi, F. Protein Translocation in Narrow Pores: Inferring Bottlenecks from Native Structure Topology. *Phys. Rev. E* **2013**, *88*, 022712.
(32) de Haan, H. W.; Slater, G. W. Translocation of "Rod-Coil" Polymers: Probing the Structure of Single Molecules within Nanopores. *Phys. Rev. Lett.* **2013**, *110*, 048101.
(33) Wong, C. T. A.; Muthukumar, M. Polymer Translocation through α-Hemolysin Pore with Tunable Polymer-Pore Electrostatic Interaction. *J. Chem. Phys.* **2010**, *133*, 045101.
(34) Chinappi, M.; Casciola, C. M.; Cecconi, F.; Marconi, U. M. B.; Melchionna, S. Modulation of Current through a Nanopore Induced by a Charged Globule: Implications for DNA-Docking. *EPL* **2014**, *108*, 46002.
(35) Bonome, E. L.; Lepore, R.; Raimondo, D.; Cecconi, F.; Tramontano, A.; Chinappi, M. Multistep Current Signal in Protein Translocation through Graphene Nanopores. *J. Phys. Chem. B* **2015**, *119*, 5815−5823.
(36) Farimani, A. B.; Heiranian, M.; Aluru, N. R. Electromechanical Signatures for DNA Sequencing through a Mechanosensitive Nanopore. *J. Phys. Chem. Lett.* **2015**, *6*, 650−657.
(37) Bernaschi, M.; Melchionna, S.; Succi, S.; Fyta, M.; Kaxiras, E. Quantized Current Blockade and Hydrodynamic Correlations in Biopolymer Translocation through Nanopores: Evidence from Multiscale Simulations. *Nano Lett.* **2008**, *8*, 1115−1119.
(38) Comer, J.; Dimitrov, V.; Zhao, Q.; Timp, G.; Aksimentiev, A. Microscopic Mechanics of Hairpin DNA Translocation through Synthetic Nanopores. *Biophys. J.* **2009**, *96*, 593−608.
(39) Jain, M.; Fiddes, I. T.; Miga, K. H.; Olsen, H. E.; Paten, B.; Akeson, M. Improved Data Analysis for the MinION Nanopore Sequencer. *Nat. Methods* **2015**, *12*, 351−356.
(40) Fologea, D.; Uplinger, J.; Thomas, B.; David, S.; McNabb, D. S.; Li, J. Slowing DNA Translocation in a Solid-State Nanopore. *Nano Lett.* **2005**, *5*, 1734−1737.
(41) Jung, Y.; Bayley, H.; Movileanu, L. Temperature-Responsive Protein Pores. *J. Am. Chem. Soc.* **2006**, *128*, 15332−15340.
(42) Timp, W.; Mirsaidov, U. M.; Wang, D.; Comer, J.; Aksimentiev, A.; Timp, G. Nanopore Sequencing: Electrical Measurements of the Code of Life. *IEEE Trans. Nanotechnol.* **2010**, *8*, 281−294.
(43) Schiel, M.; Siwy, Z. S. Diffusion and Trapping of Single Particles in Pores with Combined Pressure and Dynamic Voltage. *J. Phys. Chem. C* **2014**, *118*, 19214−19223.
(44) He, Y.; Tsutsui, M.; Fan, C.; Taniguchi, M.; Kawai, T. Controlling DNA Translocation through Gate Modulation of Nanopore Wall Surface Charges. *ACS Nano* **2011**, *5*, 5509−5518.
(45) Firnkes, M.; Pedone, D.; Knezevic, J.; Doblinger, M.; Rant, U. Electrically Facilitated Translocations of Proteins through Silicon Nitride Nanopores: Conjoint and Competitive Action of Diffusion, Electrophoresis, and Electroosmosis. *Nano Lett.* **2010**, *10*, 2162−2167.
(46) Hoogerheide, D. P.; Lu, B.; Golovchenko, J. A. A Pressure-Voltage Trap for DNA near a Solid-State Nanopore. *ACS Nano* **2014**, *8*, 7384−7391.
(47) Kowalczyk, S. W.; Wells, D. B.; Aksimentiev, A.; Dekker, C. Slowing Down DNA Translocation through a Nanopore in Lithium Chloride. *Nano Lett.* **2012**, *12*, 1038−1044.
(48) Asandei, A.; Chinappi, M.; Lee, J.; Seo, C. H.; Mereuta, L.; Park, Y.; Luchian, T. Placement of Oppositely Charged Aminoacids at a Polypeptide Termini Determines the Voltage-Controlled Braking of Polymer Transport through Nanometer-Scale Pores. *Sci. Rep.* **2015**, *5*, 10419.
(49) Jeon, B. J.; Muthukumar, M. Polymer Capture by α-Hemolysin Pore upon Salt Concentration Gradient. *J. Chem. Phys.* **2014**, *140*, 015101.
(50) Bacci, M.; Chinappi, M.; Casciola, C. M.; Cecconi, F. Role of Denaturation in Maltose Binding Protein Translocation Dynamics. *J. Phys. Chem. B* **2012**, *116*, 4255−4262.
(51) Misakian, M.; Kasianowicz, J. J. Electrostatic Influence on Ion Transport through the AlphaHL Channel. *J. Membr. Biol.* **2003**, *195*, 137−146.
(52) Wolfe, A. J.; Mohammad, M.; Cheley, S.; Bayley, H.; Movileanu, L. Catalyzing the Translocation of Polypeptides through Attractive Interactions. *J. Am. Chem. Soc.* **2007**, *129*, 14034−14041.

DOI: 10.1021/acsami.5b04406
ACS Appl. Mater. Interfaces 2015, 7, 16706−16714